Science of the Total Environment 872 (2023) 162071

Contents lists available at ScienceDirect

Science of the Total Environment

journal homepage: www.elsevier.com/locate/scitotenv

Underestimation of biomass burning contribution to $PM_{2.5}$ due to its chemical degradation based on hourly measurements of organic tracers: A case study in the Yangtze River Delta (YRD) region, China

Qing Li [a,b,1], Kun Zhang [a,b,1], Rui Li [a,b], Liumei Yang [a,b], Yanan Yi [a,b], Zhiqiang Liu [a,b,c], Xiaojuan Zhang [a,b,c], Jialiang Feng [a,b], Qiongqiong Wang [d], Wu Wang [a,b], Ling Huang [a,b], Yangjun Wang [a,b], Shunyao Wang [a,b], Hui Chen [a,b], Andy Chan [e], Mohd Talib Latif [f], Maggie Chel Gee Ooi [g], Kasemsan Manomaiphiboon [h], Jianzhen Yu [d,i], Li Li [a,b,*]

[a] School of Environmental and Chemical Engineering, Shanghai University, Shanghai, China
[b] Key Laboratory of Organic Compound Pollution Control Engineering (MOE), Shanghai University, Shanghai, China
[c] Jiangsu Changhuan Environment Technology Co., Ltd., Changzhou, Jiangsu, China
[d] Department of Chemistry, Hong Kong University of Science & Technology, Hong Kong, China
[e] Department of Civil Engineering, University of Nottingham Malaysia, Semenyih, Selangor, Malaysia
[f] Department of Earth Science and Environment, Faculty of Science and Technology, Universiti Kebangsaan Malaysia, Bangi, Selangor, Malaysia
[g] Institute of Climate Change, Universiti Kebangsaan Malaysia, Bangi, Selangor, Malaysia
[h] The Joint Graduate School of Energy and Environment, King Mongkut's University of Technology Thonburi, Bangkok, Thailand
[i] Division of Environment & Sustainability, Hong Kong University of Science & Technology, Hong Kong, China

HIGHLIGHTS

- Approximately 87 % of the levoglucosan had been degraded before sampling in Changzhou.
- Neglecting the impacts of degradations would cause a 14.9 % underestimate of OC_{BB}.
- The contribution of biomass burning to $PM_{2.5}$ is 10.7 % in Changzhou with consideration of degradation, 3.2 % higher than traditional method.

GRAPHICAL ABSTRACT

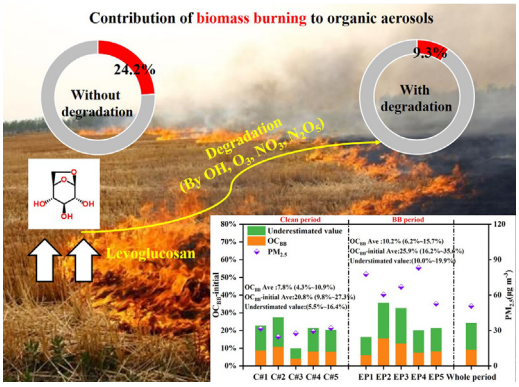

ARTICLE INFO

Editor: Jianmin Chen

Keywords:
Biomass burning
Levoglucosan
Chemical degradation
Organic tracers

ABSTRACT

Biomass burning (BB) has significant impacts on air quality and climate change, especially during harvest seasons. In previous studies, levoglucosan was frequently used for the calculation of BB contribution to $PM_{2.5}$, however, the degradation of levoglucosan (Lev) could lead to large uncertainties. To quantify the influence of the degradation of Lev on the contribution of BB to $PM_{2.5}$, $PM_{2.5}$-bound biomass burning-derived markers were measured in Changzhou from November 2020 to March 2021 using the thermal desorption aerosol gas chromatography–mass spectrometry (TAG-GC/MS) system. Temporal variations of three anhydro-sugar BB tracers (e.g., levoglucosan, mannosan (Man), and galactosan (Gal)) were obtained. During the sampling period, the degradation level of air mass (x) was 0.13,

* Corresponding author at: School of Environmental and Chemical Engineering, Shanghai University, Shanghai, China.
E-mail address: Lily@shu.edu.cn (L. Li).
[1] These two authors contributed equally to this work.

http://dx.doi.org/10.1016/j.scitotenv.2023.162071
Received 29 September 2022; Received in revised form 1 February 2023; Accepted 2 February 2023
Available online 11 February 2023

indicating that ~87 % of levoglucosan had degraded before sampling in Changzhou. Without considering the degradation of levoglucosan in the atmosphere, the contribution of BB to OC were 7.8 %, 10.2 %, and 9.3 % in the clean period, BB period, and whole period, respectively, which were 2.4–2.6 times lower than those (20.8 %–25.9 %) considered levoglucosan degradation. This illustrated that the relative contribution of BB to OC could be underestimated (~14.9 %) without considering degradation of levoglucosan. Compared to the traditional method (i.e., only using K^+ as BB tracer), organic tracers (Lev, Man, Gal) were put into the Positive Matrix Factorization (PMF) model in this study. With the addition of BB organic tracers and replaced K^+ with K^+_{BB} (the water-soluble potassium produced by biomass burning), the overall contribution of BB to $PM_{2.5}$ was enhanced by 3.2 % after accounting for levoglucosan degradation based on the PMF analysis. This study provides useful information to better understand the effect of biomass burning on the air quality in the Yangtze River Delta region.

1. Introduction

Biomass burning, defined here as the burning of plant matter in wild fires and as residential biofuel (Li et al., 2021; Yan et al., 2019), is an important source of atmospheric carbonaceous aerosol, which directly impacts air quality, visibility, cloud formation and climate (Altshuler et al., 2020; Bao et al., 2021; Feng et al., 2015; Krumal et al., 2010; Liu et al., 2019). BB is mainly divided into several categories, such as forest fires, grassland fires, fuelwood burning and agricultural residues burning (Andreae and Merlet, 2001). BB produces organic compounds such as anhydro sugar (i.e., levoglucosan, galactosan, and mannosan), aldehydes, n-alkanes and PAHs, etc., which enhance the concentrations of ozone and other gaseous pollutants, and affect atmospheric radiative balance (Chen et al., 2017).

Numerous studies have reported that levoglucosan (Lev; 1,6-anhydro-β-D-glucopyranose), a water-soluble anhydro sugar produced by thermal degradation of cellulose, can be used as a very selective tracer for BB, and has important implications for $PM_{2.5}$ source apportionment (Cheng et al., 2022; Engling et al., 2009; Fabbri et al., 2009; Fraser and Lakshmanan, 2000; Hong et al., 2022; Li et al., 2021; Simoneit, 1999; Suciu et al., 2019; van Drooge et al., 2014). The sources of Lev include open combustion (1.7 Tg $year^{-1}$) and biofuels (2.1 Tg $year^{-1}$); and its sinks include liquid-phase oxidation (2.9 Tg $year^{-1}$), non-homogeneous oxidation (0.16 Tg $year^{-1}$), gas-phase oxidation (1.4×10^{-4} Tg $year^{-1}$), dry deposition (0.27 Tg $year^{-1}$) and wet deposition (0.43 Tg $year^{-1}$) (Li et al., 2021). Lev can be oxidized in both gas (Bai et al., 2013) and aqueous phases (Suciu et al., 2019), as well as heterogeneously oxidized by gaseous oxidants (such as O_3, OH radical, NO_3 radical, and N_2O_5) on aerosol surface (Arangio et al., 2015; Li et al., 2021), which was not considered by most previous studies (Jung et al., 2014; Liu et al., 2019; Sang et al., 2011; Shen et al., 2017; Wang et al., 2020; Xu et al., 2020). For instance, in the atmosphere, levoglucosan has a lifespan of 0.7–2.2 days (typical average summertime conditions) when it is exposed to 1×10^6 molecules cm^{-3} of OH (Hennigan et al., 2010). In the aqueous phase, such as in aerosol water or cloud droplets, Lev can also be oxidized by aqueous OH (Li et al., 2021). In field measurements, significant degradation of atmospheric levoglucosan has also been reported (Hong et al., 2022; Mochida et al., 2010; Sang et al., 2012). For example, the lifetime of levoglucosan in the atmosphere is only 1.8 days when aqueous-phase chemical degradation is taken into account (Li et al., 2021). To estimate the contribution of biomass burning to $PM_{2.5}$ in the atmosphere, the ratio of levoglucosan to organic carbon (Lev/OC) is commonly utilized (Fujii et al., 2014; Hong et al., 2022; Li et al., 2021; Sang et al., 2012; Sang et al., 2013). A previous study has revealed that when levoglucosan degradation was taken into account, the estimated BB contribution to local OC may be 14 %–33 % higher than when degradation was not accounted for, which is consistent with the significant correlation between levoglucosan and OC (Li et al., 2021). Li et al. (2021) also utilized the GEOS-Chem approach to simulate levoglucosan in various locations across the world with/without considering Lev degradation pathways, which also reached a conclusion that rectification needs to be done when using measured levoglucosan in estimating its contribution to ambient particles (Li et al., 2021). Therefore, quantifying the original contribution of BB to OC [OC_{BB}] and $PM_{2.5}$ is of great significance. Although previous studies have revealed the importance of levoglucosan degradation, the reasonable contribution of BB to OC as well as $PM_{2.5}$ has been rarely investigated. In addition, most of the studies are based on filter analysis with coarse temporal resolution. Since the degradation of levoglucosan is fast, high-time resolution observations and source apportionment are of great significance to capture the quick source changes especially during BB episodes.

The Yangtze River Delta (YRD) region is one of the most economically developed metropolitan areas of eastern China, suffering from severe air pollution in recent years (Chen et al., 2022; Deng et al., 2022; Liu et al., 2022; Lv et al., 2021; Ou et al., 2022; Sun et al., 2022; Yang et al., 2022). Changzhou, located in the center of the YRD, is a representative industrialized city for the YRD region (Bi et al., 2020; Jensen et al., 2021; Ye et al., 2017). Additionally, Changzhou is also an important crop production center with a high demand of biomass disposal (Jiang et al., 2020). In this work, we investigated the hourly variations of $PM_{2.5}$-bound organic compounds during autumn and winter of 2020–2021 in Changzhou by utilizing the online thermal desorption aerosol gas chromatography–mass spectrometry (TAG-GC/MS) system, which is capable of detecting high temporal resolution levoglucosan data (He et al., 2020; Isaacman et al., 2014; Li et al., 2020; Wang et al., 2020; Williams et al., 2006; Williams et al., 2007; Zhang et al., 2021; Zhu et al., 2021). The contribution of BB to $PM_{2.5}$ was calculated using multiple methods based on measured BB tracers with/without considering Lev degradation and Positive Matrix Factorization (PMF). Spatial distribution of potential sources of anhydro sugars in BB period and clean period were obtained by utilizing the Potential Source Contribution Function (PSCF) model. The results of this study can provide critical observation evidence for policymakers in developing biomass burning control measures to improve air quality in the YRD region.

2. Methodology

2.1. Site description

The observation site is located in Changzhou Environmental Monitoring Center (119°59.730′E, 31°45.510′N), which is in the downtown of Changzhou, with several commercial streets, communities and some major traffic arteries (Zhongwu Avenue, Heping Middle Road, Guanghua Road) in the surrounding area. Changzhou is located on the Taihu Plain in the Yangtze River Delta. Plains and polder regions, the majority of which are <30 m above sea level, make up 70 % of Changzhou's total surface area (Tang et al., 2022). Geographical location and a detailed map with detailed anthropogenic sources are shown in Fig. 1. Field observation was conducted from November 1st 2020 to March 31st 2021. Observation instruments were housed on the third floor of the Monitoring Center building, with the $PM_{2.5}$ sampling spot located 1.5 m above the roof.

2.2. In-situ measurements

Hourly data of meteorological parameters (e.g., wind speed, wind direction, relative humidity, temperature, atmospheric pressure, rainfall), conventional gaseous pollutants (SO_2, NO_2, CO, O_3), particulates ($PM_{2.5}$, PM_{10}) and components of $PM_{2.5}$ (including sulfate (SO_4^{2-}), nitrate (NO_3^-), ammonium (NH_4^+), organic carbon (OC) and element carbon (EC)) during

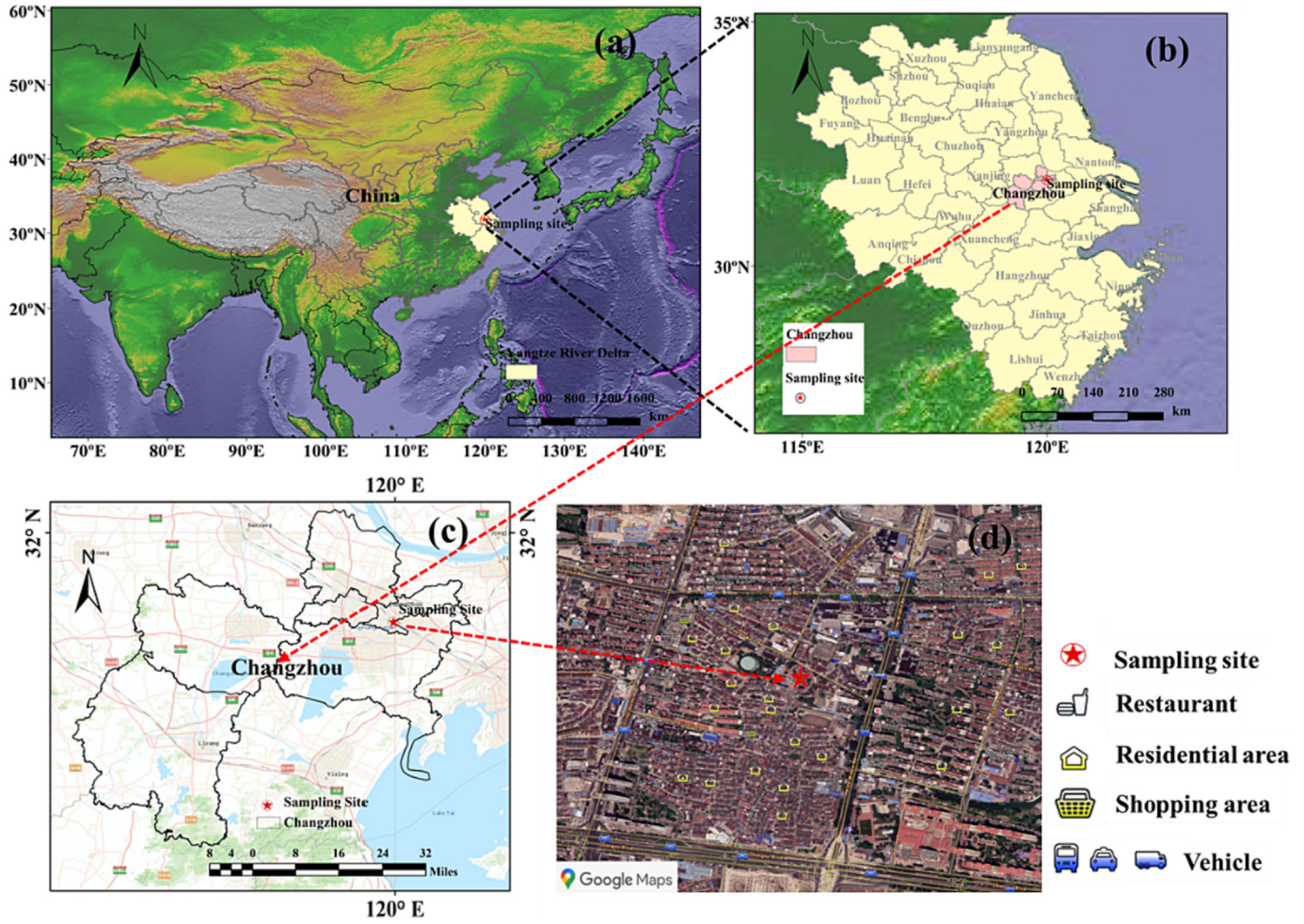

Fig. 1. Location of the sampling site.

this observation were measured. Among them, meteorological parameters were obtained by a meteorological monitor (WXT520, VAISALA Inc., FL). Concentrations of SO_2, O_3, CO, and NO/NO_2 were obtained by SO_2 analyzer (MODEL450i, Themo Fisher Scientific, US), ozone analyzer (49i-PS, Themo Fisher Scientific, US), CO analyzer (T300, API, US) and NO_x analyzer (MODEL450i, Themo Fisher Scientific, US), respectively. Both $PM_{2.5}$ and PM_{10} mass concentrations were measured by two online particulate matter monitor (BAM1020, Met One Inc., US) using β-ray method, and the concentrations of carbonaceous aerosol in $PM_{2.5}$ were measured by a semi-continuous OC/EC analyzer (RT-4, Sunset Laboratory Inc., US) using thermal light method with hourly time resolution. The concentrations of $PM_{2.5}$-bound water-soluble ions (WSIs), three anions (Cl^-, NO_3^-, SO_4^{2-}) and five cations (Na^+, NH_4^+, K^+, Mg^{2+}, Ca^{2+}) were measured using a MARGA ion online analyzer (ADI2080, Metrohm Inc., CHN) with hourly time resolution. The detection limits of the eight water-soluble inorganic ions (Cl^-, NO_3^-, SO_4^{2-}, Na^+, NH_4^+, K^+, Mg^{2+}, Ca^{2+}) measured by MARGA are 0.003, 0.009, 0.0615, 0.001, 0.0038 0.015, 0.005 and 0.025 μg. The detection limits of OC and EC are 0.0494 and 0.0285 μg, respectively. The organic markers in $PM_{2.5}$ were measured by TAG-GC/MS (Aerodyne Research Inc., USA) with bi-hourly time resolution. The detection limits of the measured sugars (Levoglucosan, Galactosan, Mannosan, Mannitol, Glucose) by TAG-GC/MS are 0.0080, 0.0052, 0.0029, 0.0094 and 0.0156 ng. The online monitoring instruments during the observation are summarized in Table S1.

The schematic diagram of the TAG-GC/MS can be found in the previously published articles from our group (Li et al., 2020; Zhang et al., 2021). A detailed description of the working principle of TAG can be found in previous publications (He et al., 2020; Isaacman et al., 2014; Li et al., 2020; Wang et al., 2020; Williams et al., 2007; Zhang et al., 2021; Zhu et al., 2021). We identified the compounds (Levoglucosan, Galactosan, Mannosan, Mannitol, Glucose) by comparing retention time and mass spectra with those of standards, and then quantified by plotting standard curves using the internal standard method. Chromatographic peaks were fitted and integrated using the TERN plug-in program based on Igor v8.04 software, with residuals of peaks <10 %. During our observation, deuterium-labeled internal standard solution was injected into each sample to monitor instrument condition and analyze contamination levels of individual species. Table S2 lists the measured organic compounds, corresponding ISs and method detection limits discussed in this study. The blank samples were collected with the entire sampling flow bypassing the denuder and the collection and thermal desorption cell (CTD), and going directly to the pump exhaust, therefore reflecting the residue in the TAG-GC/MS. Although the quantitative ion signal of the blank sample, relative to normal sampling, is negligible, we still subtracted quantitative ion signal of the blank sample from the sample runs at the same day to reduce errors.

2.3. Estimation of biomass burning contribution to aerosols using water-soluble potassium

Water-soluble potassium (K^+) has long been used as a biomass-burning tracer, but it can also be generated from sea salt and dust (Hong et al., 2022; Karavoltsos et al., 2020; Kumar et al., 2018; Li et al., 2021; Pio et al., 2008; Pio et al., 2007; Rajput et al., 2014; White, 2008). To estimate the water-soluble potassium produced by biomass burning (K^+_{BB}), we subtract the

percentage produced by sea salt and dust by the following Eqs. (1)–(5) (Engling et al., 2009; Kumar et al., 2018; Rajput et al., 2014):

$$K^{+}_{BB} = (nss - K^{+}) - (K^{+}_{Dust}) \quad (1)$$

$$nss - K^{+} = K^{+}_{aerosol} - 0.037 * Na^{+}_{aerosol} \quad (2)$$

$$K^{+}_{Dust} = 0.04 * \left[(nss - Ca^{2+}) - Ca^{2+}_{BB}\right] \quad (3)$$

$$Ca^{2+}_{BB} = nss - K^{+}/53.96 \quad (4)$$

$$nss - Ca^{2+} = Ca^{2+}_{aerosol} - 0.038 * Na^{+}_{aerosol} \quad (5)$$

where, nss-K^{+} and K^{+}_{Dust} refer to non-sea-salt-potassium and dust derived K^{+}, respectively. $K^{+}_{aerosol}$, $Na^{+}_{aerosol}$ and $Ca^{2+}_{aerosol}$ represent concentrations of potassium, sodium and calcium in aerosol samples. The calculation of the minimum and maximum nss-(K^{+}/Ca^{2+}) ratios was described in detail in Text S1 and Fig. S1. The minimum and maximum nss-(K^{+}/Ca^{2+}) ratios of 0.04 and 54 (=53.96 + 0.04) have been utilized to deduce the K^{+}_{BB}. A sea-salt-(K^{+}/Na^{+}) mass percentage of 0.037 and a sea-salt-(Ca^{2+}/Na^{+}) mass ratio of 0.038 were adopted from the literature for sea-salt correction (Kumar et al., 2018; Pio et al., 2007; Rajput et al., 2014). This applies to sites affected by marine aerosols.

2.4. Contribution of biomass burning to organic carbon with/without consideration of chemical degradation of levoglucosan

Levoglucosan has been employed as a molecular tracer in a number of prior investigations to quantify the contribution of BB to OC (OC_{BB}) (Hong et al., 2022; Li et al., 2021), which can be represented as:

$$OC_{BB} = \frac{(Lev/OC)ambient}{(Lev/OC)source} \times 100\% \quad (6)$$

where the $(Lev/OC)_{ambient}$ and $(Lev/OC)_{source}$ represent the Lev/OC ratios in ambient and biomass burning source emission, respectively. Due to inadequate source profiles for constituent ratios of different types of biomass in different seasons under actual ambient situations, 0.082 was reported as the (Lev/OC) source ratio for $PM_{2.5}$ (Zhang et al., 2007). An average levoglucosan to OC ratio of 8.2 % from a combustion chamber study was first used in biomass burning source emission studies for three primary types of cereal straw (corn, wheat, and rice) in China (Zhang et al., 2007). This value can be used in combination with the (Lev/OC) ambient ratios of our $PM_{2.5}$ samples to roughly estimate the contribution of biomass burning to the ambient OC. This method has been widely used to quantify the contribution of BB to OC and 0.082 is a universal value that has been applied in many literatures. (Liu et al., 2019; Sang et al., 2011; Zhang et al., 2014).

The OC_{BB}-initial in Changzhou can be quantified with the concentration of levoglucosan without chemical degradation by the following Eq. (7)–(9):

$$OC_{BB} - inital = \frac{(Lev\_no - chem/OC)ambient}{(Lev/OC)source} \times 100\% \quad (7)$$

$$Lev\_no - chem = \frac{(Lev)ambient}{x} \quad (8)$$

$$x = 0.18 \times \frac{(Lev)ambient}{(K^{+}_{BB})ambient} + 0.08 \quad (9)$$

where the values of 0.18 and 0.08 were the slope and intercept of the modeled Lev/Lev_no-chem, employing the Levoglucosan/K^{+}_{BB} value in global with a various underlying surface (including urban, rural, forest, marine, and polar, $R = 0.84$) (Li et al., 2021); OC_{BB}-initial stands for the initial contribution of BB to OC; Lev_no-chem represents levoglucosan without chemical degradation. There are uncertainties in the Lev_no-chem obtained by the calculation, mainly due to the slope in Eq. (9). In this study, we took into consideration that chamber experiments differentiate from atmospheric processing aerosols. Therefore, we conducted uncertainty analysis of the calculation. To analyze the uncertainty of the slope, the slopes plus ±10 % and ± 20 % are discussed to calculate the Lev_no-chem and its use as a tracer of biomass combustion. The contribution of BB to $PM_{2.5}$, OC and EC was evaluated using PMF model in the ranges of 10.7 % ~ 11.0 %, 38.9 % ~ 39.4 %, and 44.3 % ~ 44.7 %, respectively (Table S3), suggesting negligible influence of the uncertainty of the slope on the results. Therefore, when the uncertainty range of the slope is −10 % ~ 20 %, the effect on the results can be neglected.

Where x (Eq. 9) refers to the degradation level of air mass. Owing to the fact that K^{+}_{BB} is relatively stable in the atmosphere. In Eq. (9), the x values can change from 0 to 1. If the x value and $(K^{+}_{BB})_{ambient}$ (Eq. 9) are equal to 1, this suggests a totally fresh levoglucosan in the atmosphere. From Table S4, the mean value of x in the whole period, clean period, and BB period was 0.13 ± 0.07 (ranging from 0.08 to 1.04), 0.11 ± 0.03 (ranging from 0.08 to 0.21), 0.14 ± 0.06 (ranging from 0.08 to 0.60), respectively. The mean value of x during BB period was higher than the clean period, indicative of fresher levoglucosan emissions due to the influence of biomass burning (Hong et al., 2022). As a conclusion, the degradation of levoglucosan had to be taken into account in this study.

2.5. Contribution of biomass burning to aerosols based on different methods

To investigate the contribution of BB to OC, M1 and M2 based on ratios of BB tracers were discussed, without and with considering the degradation of levoglucosan, respectively. The calculation method is described in detail in Eqs. (6)–(9). These two methods were used to assess the contribution of BB to OC.

To deeply investigate the contribution of BB to $PM_{2.5}$, A1-A4 applied the PMF model (version 5.0). With time series of $PM_{2.5}$, carbonaceous aerosols (OC and EC), water-soluble inorganic ions (Cl^{-}, NO_3^{-}, SO_4^{2-}, NH_4^{+}, Na^{+}, Mg^{2+}, Ca^{2+} and K^{+}), inorganic elements (Si, Fe, Ni, Se, As, Zn, Cr, V, Mn, Pb, Ba, Cu and Ti), and levoglucosan, galactosan, mannosan are used as input data. Carbonaceous aerosols, water-soluble inorganic ions, and inorganic elements were input in A1, where K^{+} was used as a tracer for BB. A2 replaced K^{+} with K^{+}_{BB}. Anhydro sugars were input in A3 and A4, and the degradation of levoglucosan was considered in A4. A3 didn't consider the degradation of levoglucosan. The species used in the PMF model are shown in Table 1. The uncertainty of each data input in the PMF model was calculated according to Eq. (10):

$$u_{ij} = \sqrt{(x_{ij} \times EF)^2 + \left(\frac{1}{2} \times MDL\right)^2} \quad (10)$$

where MDL is the method detection limit and EF is the error fraction determined by the user and associated with the measurement uncertainties. x_{ij} is concentration of compound j in the receptor environment at hour i; u_{ij} is uncertainty of compound j concentration in the receptor environment at hour i. The concentration data below MDL was replaced by 0.5 of the MDL, and the corresponding uncertainty u_{ij} was calculated by five-sixths of the MDL. Missing values were replaced by the median value of the species, and its u_{ij} was assigned as four times of the median value (Norris et al., 2014).

2.6. Backward air mass trajectory analysis

To identify various source regions of pollutants arriving at Changzhou in BB period and Clean period, 48-h backward trajectories, arriving at the height of 500 m (above ground level) at the sampling site were calculated by the HYSPLIT model (http://ready.arl.noaa.gov/HYSPLIT.php) (Wang et al., 2009). Afterwards, the cluster analysis of air mass trajectories was performed using the cluster calculation module. A reasonable maximum cluster number can be decided through visual inspection and diagnostic parameters (Text S2 and Fig. S2). Furthermore, PSCF analysis was used on a

Table 1
Contribution of biomass burning to aerosols based on different methods.

Methods	BB to $PM_{2.5}$	BB to OC	BB to EC	Other sources to $PM_{2.5}$ by PMF	R	Input species	Purpose
M1: Based on ratios of tracers (without considering the degradation of Lev)	–	9.3 %	–	–	–	(**Lev**/OC)ambient and (**Lev**/OC)source	Base
M2: Based on ratios of tracers (considering the degradation of Lev)	–	24.2 %	–	–	–	(**Lev**/OC)ambient, (Lev/OC)source, $\mathbf{K^+_{BB}}$, and *x* (The ratio of aging in air masses))	Validation of the effects of chemical degradation
A1:By PMF(with BB tracers K^+)	16.7 %	42.5 %	40.6 %	Secondary aerosols (55.0 %), industrial emission (12.5 %), coal combustion (2.4 %), dust (10.3 %), and fireworks (3.0 %)	0.94	($PM_{2.5}$, OC, EC, Cl^-, NO_3^-, SO_4^{2-}, NH_4^+, Na^+, Mg^{2+}, Ca^{2+}, **K^+**, Si, Fe, Ni, Se, As, Zn, Cr, V, Mn, Pb, Ba, Cu, and Ti)	Base
A2: By PMF (with BB tracer K^+_{BB})	16.3 %	41.4 %	39.8 %	Secondary aerosols (55.0 %), industrial emission (12.6 %), coal combustion (2.5 %), dust (10.5 %), and fireworks (3.0 %)	0.94	($PM_{2.5}$, OC, EC, Cl^-, NO_3^-, SO_4^{2-}, NH_4^+, Na^+, Mg^{2+}, Ca^{2+}, $\mathbf{K^+_{BB}}$, Si, Fe, Ni, Se, As, Zn, Cr, V, Mn, Pb, Ba, Cu, and Ti)	Deducting the effect of K^+ from ocean and dust
A3: By PMF (with BB tracers K^+_{BB} and anhydro sugars, without considering the degradation of Lev)	7.5 %	35.9 %	40.5 %	Secondary aerosols (53.8 %), industrial emission (19.7 %), coal combustion (6.6 %), dust (10.1 %), and fireworks (2.1 %)	0.95	($PM_{2.5}$, OC, EC, Cl^-, NO_3^-, SO_4^{2-}, NH_4^+, Na^+, Mg^{2+}, Ca^{2+}, $\mathbf{K^+_{BB}}$, Si, Fe, Ni, Se, As, Zn, Cr, V, Mn, Pb, Ba, Cu, Ti, **Lev, galactosan, mannosan**)	Adding organic and inorganic tracers to resolve the contribution of biomass burning to aerosol
A4: By PMF (with BB tracers K^+_{BB} and anhydro sugars, considering the degradation of Lev)	10.7 %	39.1 %	44.5 %	Secondary aerosols (55.8 %), industrial emission (14.1 %), coal combustion (2.4 %), dust (13.6 %), and fireworks (3.4 %)	0.96	($PM_{2.5}$, OC, EC, Cl^-, NO_3^-, SO_4^{2-}, NH_4^+, Na^+, Mg^{2+}, Ca^{2+}, $\mathbf{K^+_{BB}}$, Si, Fe, Ni, Se, As, Zn, Cr, V, Mn, Pb, Ba, Cu, Ti, **Lev_no-chem, galactosan, mannosan**)	Validation of the effects of chemical degradation

Note:R is correlation coefficient between $PM_{2.5}$ measured and $PM_{2.5}$ simulated by PMF; BB tracers font were bolded.

0.25° × 0.25° grid to investigate the variability of potential source regions of anhydro sugars on BB period and clean period.

3. Results and discussion

3.1. Overview of the field campaign

During the campaign, the mass concentration of $PM_{2.5}$ ranged from 3 to 218 μg m^{-3}, with an average value of 50.8 ± 27.9 μg m^{-3} (Fig. 2 and Table S5). The characteristics of other conventional pollutants were described in detail in Text S3. According to Fig. 2 and Fig. S3, $PM_{2.5}$ level in Changzhou has a certain periodicity, and the frequency of pollution events is about once a week. Furthermore, secondary formation was the dominant source of heavy pollution throughout the observation period (Text S4), with nitrate being the most prominent (34 %, mass percentage, same below) and organic matter (i.e., OM = OC*1.6, 21.8 %) (Li et al., 2020) being the second greatest of $PM_{2.5\_reconstructed}$, respectively (Table S5, Fig. S6). The concentrations of water-soluble ions (WSIs) followed $NO_3^- > NH_4^+ > SO_4^{2-} > Cl^- > K^+ > Ca^{2+} > Na^+ > Mg^{2+}$, with secondary inorganic aerosols (sulfate, nitrate and ammonium, i.e., SNA) constituted a majority (~91.1 %) of WSIs mass.

The clean periods (C#1 (2021-01-12), C#2 (2021-02-09 ~2021-02-10), C#3 (2021-02-17), C#4 (2021-03-01 ~2021-03-03) and C#5 (2021-03-06 ~2021-03-07)) were filtered when the daily concentrations of $PM_{2.5}$ were <35 μg m^{-3}(green dashed frame in Fig. 2). Considering the lifetime of levoglucosan, which is around 0.7–2.2 days (Hennigan et al., 2010), we define the BB event when the 48-h average concentration of anhydro sugar (Lev + Gal + Man) is >50 ng m^{-3} and a peak concentration exceed 100 ng m^{-3} in this study. Five BB episodes (EP1 (2020-11-06 ~2020-11-08), EP2 (2021-01-13 ~2021-01-14), EP3 (2021-01-31 ~2021-02-04), EP4 (2021-03-13 ~2021-03-16) and EP5 (2021-03-24 ~2021-03-25)) were identified over the whole observation period, and were marked with red dashed frame in Fig. 2. The average total concentration of anhydro sugars measured in the five episodes were 61.1, 250.5, 114.2, 54.5 and 82.6 ng m^{-3}, respectively. In the study, the differences in the averages provided are statistically significant (Text S5). In particular, SO_4^{2-}, NO_3^-, NH_4^+, and secondary organic carbon (SOC) showed relatively higher concentrations during BB period (Table S5), exceeding those in the clean period by factors of 1.4, 2.4, 2.0, and 2.1, indicating an enhanced formation of secondary aerosols during the BB period. The higher concentrations of SOC in BB period could be attributed to the spontaneous oxidation of levoglucosan in the atmosphere (Bai et al., 2013). The average aerosol water content (AWC, detailed description in Text S6) during BB period (21.2 ± 22.5 μg m^{-3}) is also higher than that in clean period (13.6 ± 15.3 μg m^{-3}). Given the higher AWC during the BB period, and a more positive correlation (= 0.84 ~ 0.86, $p < 0.01$) found between secondary inorganic aerosols and AWC (Fig. S9), heterogeneous reactions could play a significant role in the secondary aerosol formation and the degradation of Lev in the atmosphere.

3.2. Characteristics of BB-related saccharides

According to the summary results of previous studies listed in Table S6, due to biomass burning (Hong et al., 2022; Krumal et al., 2010; Xiao et al., 2018; Xu et al., 2020; Zhu et al., 2015), the concentrations of anhydro sugars (levoglucosan, galactosan, mannosan, i.e., BB-related saccharides) were slightly higher in winter than that in summer, while biomarkers (including mannitol and glucose) were more abundant in warm seasons, which is attributed to the active biological emissions (Xiao et al., 2018; Xu et al., 2020). Fig. S10 shows the concentration distribution of individual saccharides species and their average contribution to total saccharides in Changzhou. The average concentrations of levoglucosan, galactosan and mannosan were 54.2 ± 80.2, 2.7 ± 3.0 and 4.3 ± 5.6 ng m^{-3}, respectively. Levoglucosan accounted for 80.1 % of the total BB-related saccharides, and the average concentration was slightly higher than that reported in Shanghai (45.9 ng m^{-3}) (Wang et al., 2020) at the same

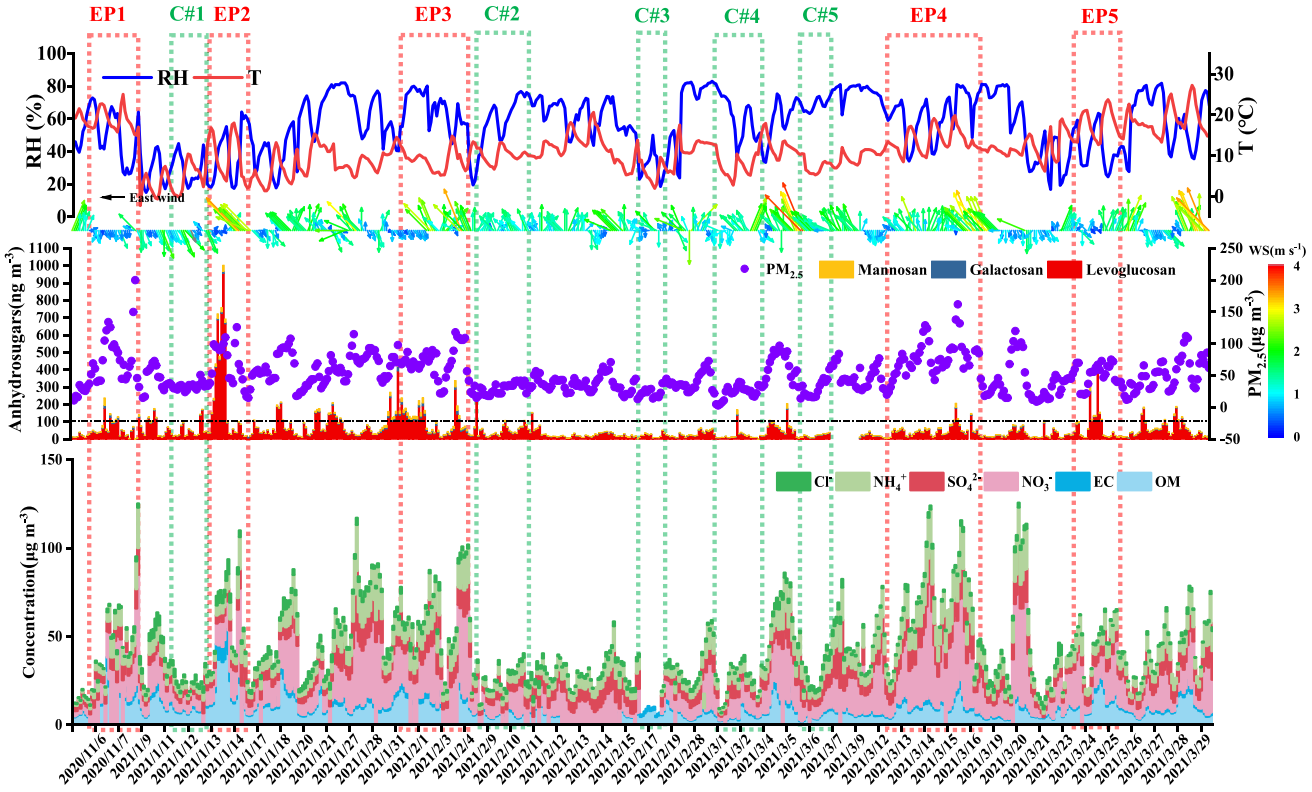

Fig. 2. Time series of meteorological conditions, anhydro sugars, Cl^-, NH_4^+, SO_4^{2-}, NO_3^-, EC, OM, and $PM_{2.5}$ during the observation period.

study period. Especially, the BB-related anhydro sugars (104.2 ± 141.5 ng m^{-3}), levoglucosan (91.4 ± 133.1 ng m^{-3}), Lev_no-chem (601.2 ± 645.2 ng m^{-3}), galactosan (4.7 ± 4.6 ng m^{-3}), and mannosan (8.1 ± 8.6 ng m^{-3}) showed relatively higher concentrations during the BB period, exceeding those in the clean period by factors of 2.4–3.5 (Table S5). These results suggested a considerable increase in anhydro sugars during biomass burning events. To evaluate the impact of BB on fine particulate and the potential aging of levoglucosan, the ratios of levoglucosan to OC (Lev/OC) and EC (Lev/EC) were used (Xu et al., 2020). The mean value of Lev/OC in the BB period (0.85 ± 0.63 %) was higher than in the clean period (0.64 ± 0.38 %), indicating that the influence of biomass burning was stronger during the BB period. The Lev/EC ratios exhibited maxima in BB period (0.03 ± 0.02), relatively higher than that in clean period (0.02 ± 0.01), further supports that biomass combustion has a significant impact on aerosol composition.

According to Fig. S11 and Fig. S12, the absolute concentrations of ambient anhydro sugars could be influenced by other factors (e.g., relative humidity, wind speed, temperature, aerosol water content (AWC), etc.) in addition to biomass burning. The BB-related anhydro sugars were negatively correlated with wind speed ($r = -0.3 \sim -0.6$) and temperature ($r = -0.3 \sim -0.5$), but exhibited a positive correlation with AWC ($r =$ 0.3– 0.5) and relative humidity ($r =$ 0.3– 0.5) during the BB period (Fig. S12). The saccharides showed a double peak in the morning and evening (Fig. S11), with high relative humidity and low wind speed in the morning and evening, which is favorable to the accumulation of pollutants. Moreover, the higher values of AWC in the morning and evening are favorable to the aqueous-phase processes as well as heterogeneous oxidation for levoglucosan (Li et al., 2021).

3.3. Source identification of biomass burning based on diagnostic parameters

The quantity of anhydro sugars in particulate matter varies by season, and the composition of the major tracer compounds in $PM_{2.5}$ produced by combustion of different types of biomass burning also varies (Cheng et al., 2013). The Lev/Man ratios from crop residue burning could be >40, while it could be in the range of 15–25, and 3–10 for hardwood and softwood burning, respectively (Cheng et al., 2013; Engling et al., 2009; Fu et al., 2012; Fu et al., 2016; Sang et al., 2013; Xu et al., 2020). The average Lev/Man ratios in the whole period, clean period, and BB period were 14.1 ± 6.6 (ranging from 0.3 to 47), 14.07 ± 5 (ranging from 0.9 to 26.3) and 12.7 ± 7.5 (ranging from 3.4 to 47) (Table S5), respectively, suggesting that the dominant burning substrates were a mixture of softwood and hardwood. Compared to the clean period (2.3 ± 3 ng m^{-3}) and the whole period (4.3 ± 5.6 ng m^{-3}), the mean value of mannosan was highest during the BB period (8.1 ± 8.6 ng m^{-3}) (Table S5). Therefore, the average Lev/Man ratio in BB period was lower than the other periods. The ratio of mannosan to galactosan (Man/Gal) is used as an auxiliary method to distinguish the burning substrates because mannosan is more abundant than galactosan in combustion smokes of crop straws, grasses and briquettes (Fabbri et al., 2009; Vicente et al., 2018; Xu et al., 2020). The average of Man/Gal ratios in the whole observation, BB cases and clean periods were 1.62 ± 1.03 (ranging from 0.4 to 21.3), 2.0 ± 1.7 and 1.4 ± 0.4 (Table S5), respectively, consistent with the higher abundance of mannosan over galactosan associated with the BB products from crop wastes in the North China Plain (Fu et al., 2008; Xu et al., 2020).

The biomass burning characteristics, expressed in the parameter space of Lev/Man and Lev/K^+ in Fig. 3, are used to differentiate the burning substrates. The ratio space for needle, duff, hardwood, softwood and crop residuals was introduced by the work of Cheng et al. (2013), which overcomes the limitation of using only one characteristic ratio (either Lev/K^+ or Lev/Man) to distinguish the types of biomasses being burned and hence increases the reliability of determination (Cheng et al., 2013). Previous studies have shown that emissions from the combustion of crop residuals such as rice straw, wheat straw and corn straw exhibit comparable levoglucosan to K^+ ratios, typically below 1.0 and a higher Lev/Man ratio which was reported to be 20–41 (Cheng et al., 2013; Liu et al., 2019). Without considering the degradation of levoglucosan, the mean ratio of Lev/K^+ was 0.22 ± 0.25 during the whole observation (Fig. 3a), with higher values in the BB period (0.32 ± 0.29), but lower ratios in the clean period (0.17 ± 0.34). Our Lev/K^+ ratios fell within the range of

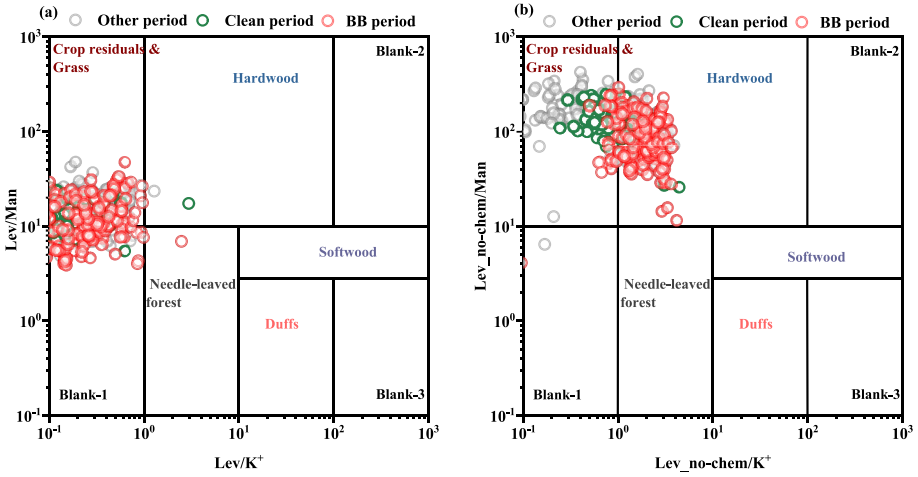

Fig. 3. Scatter plot of Lev/K^+ versus Lev/Man (a) and Lev_no-chem/K^+ versus Lev_no-chem/Man (b) of different types of biomass burning introduced by Cheng et al. (2013) and results from the ambient samples collected in this study.

those in the burning of crop straws, suggesting that most of BB aerosol was also contributed by the burning of crop straws. Particularly, during the BB period, positive correlation was found between levoglucosan and K^+ (r = 0.81, $p < 0.01$) (Fig. S8), which is another BB tracer. Consistently, levoglucosan and K^+ were weakly correlated during clean period (r = 0.36).

By considering the degradation of levoglucosan, the mean ratio of Lev_no-chem/K^+ was estimated to be 1.46 ± 0.86. The average of Lev_no-chem/K^+ ratio in the BB period (2.0 ± 0.82) was much higher than the clean period (1.16 ± 0.78) (Fig. 3b). Compared with previous studies, such ratios were higher than those of straw burning (0.1–0.6), but lower than those discovered with wood burning (5.9–23.9) (Engling et al., 2006; Fushimi et al., 2017; Zhang et al., 2007). This suggested that the BB aerosol was mainly emitted by mixed sources of burning from wood and straw residuals, and it was much more scientific to consider the chemical degradation of levoglucosan (Hong et al., 2022; Li et al., 2021; Liu et al., 2019; Mochida et al., 2010).

3.4. Impact of levoglucosan degradation on BB contribution to carbonaceous aerosols

Due to the degradation of Lev, the contribution of BB to OC at the receptor site might be underestimated. During the sampling period, the degradation level of air mass (x) was 0.13 ± 0.07 (ranging from 0.08 to 1.04), indicating that ~87 % of levoglucosan on average had been degraded before sampling in Changzhou. The x estimated in Changzhou was comparable to that reported by a previous study in wintertime Changchun (0.17) (Hong et al., 2022). Considering the degradation effects, the average concentration of Lev_no-chem in whole period was estimated to be 418.3 ± 422.2 ng m^{-3} in this work, which was 7.7 times higher than Lev_measured (54.2 ± 80.2 ng m^{-3}) (Fig. 4a). Such results reflected that degradation could significantly impact the concentration of levoglucosan in particulate matter.

To quantitatively analyze the influence of BB to carbonaceous aerosols, the chemical degradation of levoglucosan were considered, with detailed information and results given below:

M1: Based on ratios of BB tracers, without consideration of the degradation effects of levoglucosan, the average fraction of OC_{BB} was 9.3 ± 6.2 % (0–43 %), with the highest level in the BB period (10.2 ± 7.6 %), followed by clean period (7.8 ± 4.5 %) (Fig. 4b).
M2: Based on ratios of BB tracers, with consideration of the degradation of levoglucosan, the OC_{BB}-initial fractions ranged from 0.5 % to 94.2 % (Fig. S13), with a mean value of 24.2 ± 15.4 %. The significant variations of OC_{BB}-initial were found with the highest levels in the BB period (25.9 ± 18.0), followed by clean period (20.8 ± 11.8). As shown, without consideration of levoglucosan degradation, the contributions of BB to OC would be underestimated by 5.5 % ~ 19.9 % across different periods. Comparing to M1, without considering the degradation of levoglucosan would lead to underestimation of BB to OC by 14.9 % during the whole campaign. The ratio of OC_{BB}-initial was in agreement with those estimated by applying Eqs. (7)–(9) to correct for levoglucosan's degradation in Lin'an (14 % ~ 33 %) (Li et al., 2021). However, our OC_{BB}-initial value in Changzhou was lower than that in Zhengzhou (~36.8 %) (Chen et al., 2018), Changchun (~42.3 %) (Hong et al., 2022) and Daejeon (~45 %) (Jung et al., 2014). The higher contribution of biomass combustion in Zhengzhou might be attributed to the local open burning activity (Chen et al., 2018). According to Fig. S14, the daily characteristics of Lev, Lev_no-chem, OC_{BB} and OC_{BB}-initial showed early and late bimodal peaks with consistent trends.

3.5. Contribution of biomass burning to $PM_{2.5}$ with considering the degradation of levoglucosan by PMF

To quantitatively analyze the influence of BB to $PM_{2.5}$, OC and EC, the PMF model were applied (Table 1 and Text S7), with detailed information and results given below:

A1: With time series of $PM_{2.5}$, OC, EC, Cl^-, NO_3^-, SO_4^{2-}, NH_4^+, Na^+, Mg^{2+}, Ca^{2+}, K^+, Si, Fe, Ni, Se, As, Zn, Cr, V, Mn, Pb, Ba, Cu and Ti from field campaign as inputs species in the PMF model, the contribution of BB to $PM_{2.5}$, OC, and EC is 16.7 %, 42.5 %, and 40.6 %, respectively. A2-A4 are based on analysis of this investigation.
A2: In the purpose of deducting the effect of K^+ from ocean and dust, on the basis of A1, K^+_{BB} instead of K^+, the contribution of BB to $PM_{2.5}$, OC, and EC was estimated to be 16.3 %, 41.4 % and 39.8 %, respectively. By comparing A2 and A1, it demonstrates that the K^+ from the ocean and dust may lead to an overestimation of BB to $PM_{2.5}$, OC, and EC by 0.4 %, 1.1 %, and 0.6 % in the results of A1, respectively.
A3: Adding organic tracers to resolve the contribution of BB to aerosol, organic tracers (levoglucosan, galactosan, mannosan) were put into the PMF model. The addition of organic tracers could effectively identify BB and reduce interference from other sources. Without considering the degradation of levoglucosan, the contribution of BB to $PM_{2.5}$, OC, and EC is 7.5 %, 35.9 %, and 40.5 %, respectively.
A4: On the basis of A3, considering the degradation of levoglucosan, the contribution of BB to $PM_{2.5}$, OC, and EC is 10.7 %, 39.1 %, and 44.5 %, respectively. Comparison of A3 and A4, without considering the degradation of levoglucosan, led to underestimation of BB to $PM_{2.5}$ by 3.2 % during the whole campaign; Comparison of A2 and A4, using only inorganic

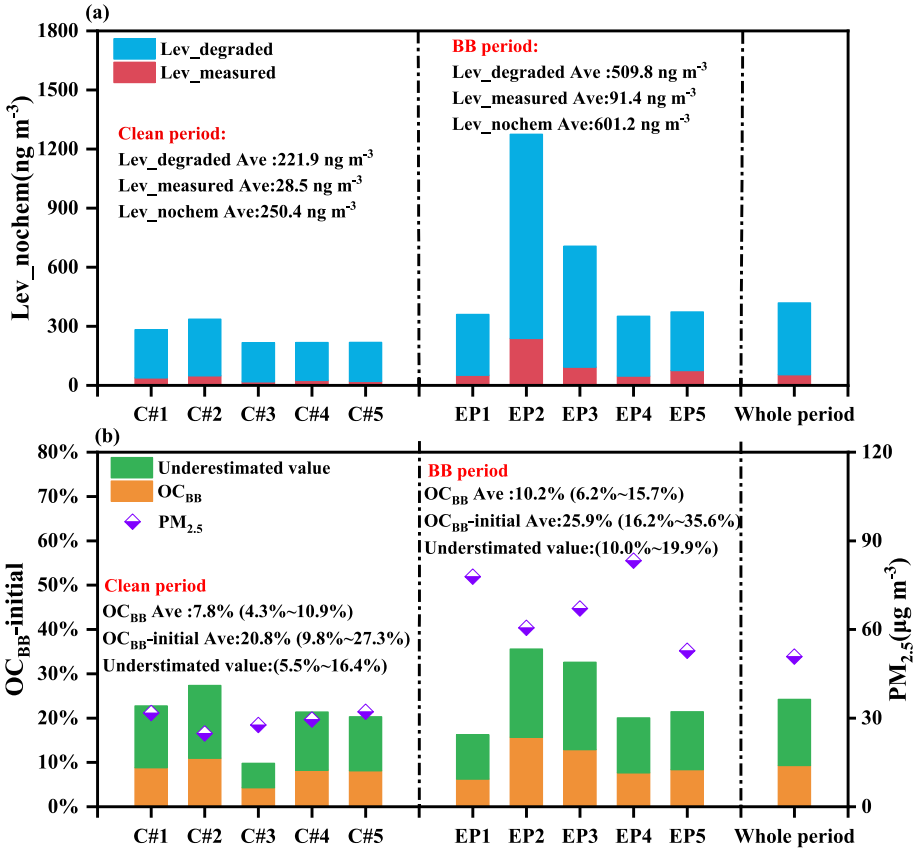

Fig. 4. Degradation of levoglucosan (a) and the contribution of BB to OC (b) in different period, where underestimated value is [OC_{BB}-initial]-[OC_{BB}].

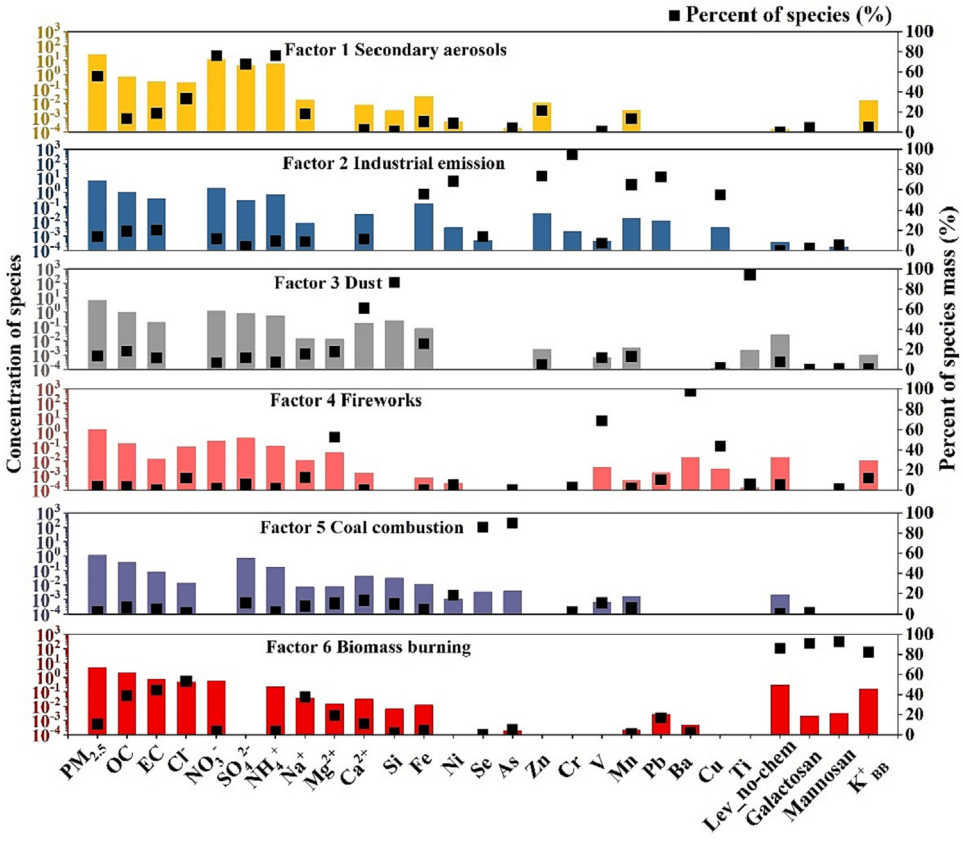

Fig. 5. Factor profiles (with BB tracers K^+_{BB} and anhydro sugars) based on the results of A4 and resolved by PMF.

tracers (K^+) and without organic tracers (i.e., levoglucosan, galactosan, mannosan) in the A2, led to overestimation of BB to $PM_{2.5}$, and OC by 6.0 %, and 3.4 %, respectively.

In A4, the PMF analysis identified 6 pollution sources, including one secondary-source factor (i.e., secondary aerosols (55.8 %) and 5 primary sources (i.e., industrial emission (14.1 %), dust (13.6 %), biomass burning (10.7 %), coal combustion (2.4 %), and fireworks (2.3 %) (Fig. 5 and Table 1).

The secondary aerosol factor (factor 1) is identified by high contributions of nitrate, sulfate, and ammonium (76.0 %, 67.7 % and 76.3 %, respectively), contributing 55.8 % to $PM_{2.5}$. Secondary aerosols make the highest contribution to local $PM_{2.5}$ based on the results of A4. From the results of A1-A3, it could also be noticed that secondary aerosols dominate with a range of 53.8 %–55.0 % (Table 1).

The profile of factor 2 contains high loadings of Cr (94.8 %), Zn (73.4 %), Pb (72.5 %), Ni (68.0 %), Mn (64.7 %), Fe (55.2 %) and Cu (54.4 %). Cr is widely used in industrial activities such as plating operation, tanning industry, chromate reduction and metallurgy (Karar et al., 2006). The enrichment of metallic elements such as Cr, Zn, Ni, Mn, Pb, Fe and Cu indicates that this factor is related to industrial production activities. Furthermore, industrial emissions are the largest primary source of emissions in Changzhou, contributing14.1 % to $PM_{2.5}$ in factor 2.

The dust factor (factor 3) is distinguished by Ca^{2+} and other crustal elements (Si, Fe and Ti). It is inferred that this type of source is mainly related with road dust, site dust, sand and construction dust. The average contribution of dust sources to $PM_{2.5}$ is 13.6 %. Especially, In the evening (18:00–22:00), this type of source contributes more and is mostly driven by evening peak traffic and an increase in heavy trucks operations (Fig. 6).

Factor 4 contains abundant of Ba (97.6 %), V (69.2 %), Mg^{2+} (52.6 %), and Cu (43.8 %). They all have a flame color reaction, tracing for fireworks. Besides, emissions from this category of sources are mainly concentrated during the Chinese New Year (February 11th–17th, 2021), with less emissions during other periods. Emission characteristics are mainly concentrated at night from 20:00 till midnight, in accordance with the characteristics of the customary activities of Chinese New Year.

Factor 5 contains a high abundance of As and Se, and >80 % of As and Se were found in this factor, which indicates this factor to be associated with coal combustion. In the previous study, residential coal combustion was listed as a source of levoglucosan in China (Yan et al., 2018). However, in this study, levoglucosan have a low load in coal combustion, and the addition of its isomers (galactosan and mannosan) from biomass combustion can effectively distinguish between coal combustion and biomass burning in PMF model.

Factor 6 is characterized by high loadings of Lev_no-chem, galactosan, mannosan and K^+_{BB}. In addition, this type of source also contains a certain proportion of OC, EC, and Cl^-, etc. Anhydro sugars (levoglucosan, galactosan and mannosan) and K^+_{BB} are uniquely emitted by biomass burning activities (Hong et al., 2022; Li et al., 2021; Liu et al., 2019; Rajput et al., 2014), thereby serving as reliable source tracers of biomass burning. It accounts for 10.7 % of the total $PM_{2.5}$ in Changzhou, which is in agreement with Shanghai (BB to $PM_{2.5}$:12.3 %) studied by other group (Feng et al., 2022). The diurnal variation in biomass burning shows higher contributions during the nighttime (Fig. 6).

3.6. BB contribution to $PM_{2.5}$ under different air mass trajectories and potential source contribution factor analysis

Here, on the basis of A4, considering the degradation of levoglucosan, the contribution of BB to $PM_{2.5}$ can reflect the original situation in the atmosphere. As shown in Fig. 7, the backward trajectories at Changzhou during the BB period and clean period were classified into 5 and 4 different air clusters. Table S7 summarizes the percentages of each trajectory cluster in BB period and clean period, and the corresponding concentrations of chemical components in ambient $PM_{2.5}$. The mean pollutant concentration in each cluster can be computed using the cluster statistics function by TrajStat 1.5.3 (http://meteothink.org/downloads/index.html). Pollutant pathways could then be associated with the high concentration clusters. During the BB period, the air mass trajectories were mainly from the southwest (39.1 % from Cluster1), north (19.8 % from Cluster2), and northwest (15.6 % from Cluster4) continental air masses of the sampling site (Fig. 7a), and there are more fire points where it passes (Fig. S15). The contribution of BB to $PM_{2.5}$ in Cluster 1–5 during BB period is ranked as Cluster4 (23.2 %) > Cluster1(17.2 %) >

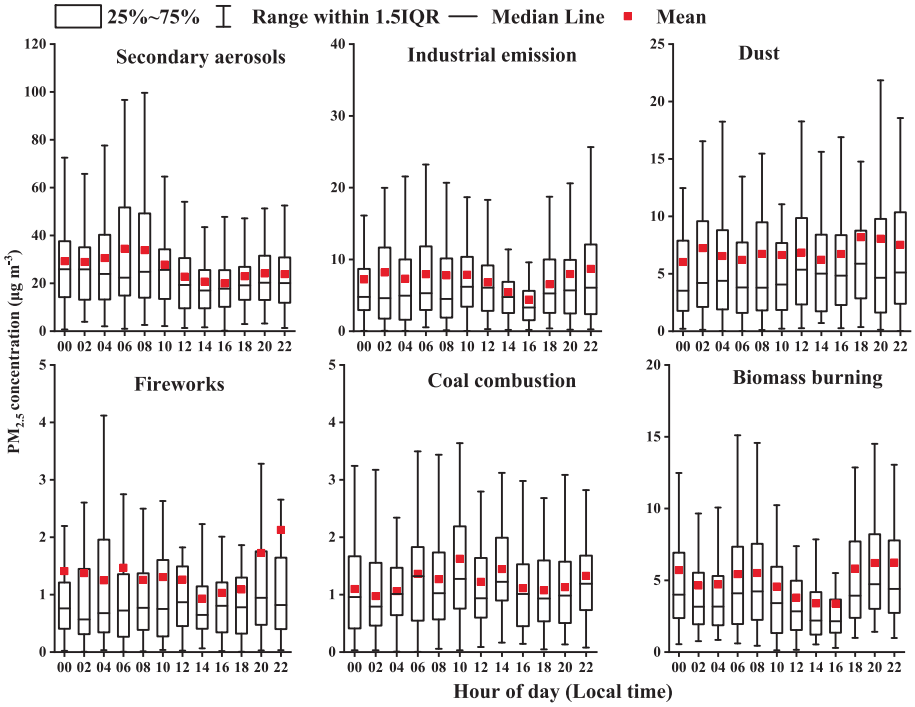

Fig. 6. Diurnal variation in individual source factors based on the results of A4 and resolved by PMF.

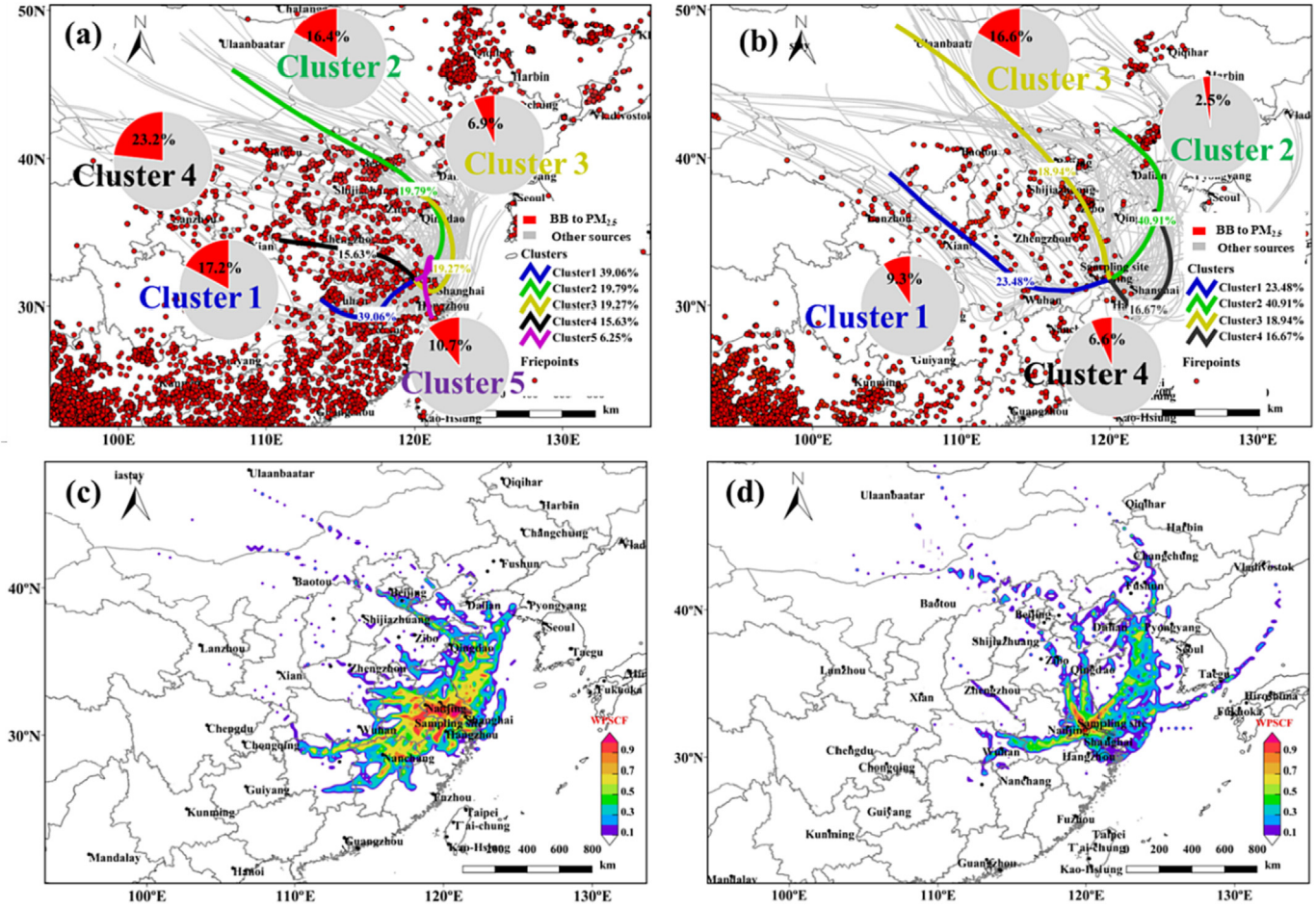

Fig. 7. The potential source results based on the results of A4. Backward trajectory analysis in BB period (a) and clean period (b) during the Campaign. The red dot in the maps indicates the fire points, the size of the red pie chart represents sources of $PM_{2.5}$ (red pie chart represents the contribution of BB to $PM_{2.5}$, gray pie chart represents other sources of $PM_{2.5}$) in each cluster, and potential source contribution function (PSCF) analysis of anhydro sugars in BB period (c) and clean period (d). Moreover, the fire spots data were acquired from the MODIS satellites through the Fire-Map website of NASA (www.firms.modaps.eosdis.nasa.gov/map/).

Cluster2 (16.4 %) > Cluster5 (10.7 %) > Cluster3 (6.9 %) (Fig. 7a). To mitigate the $PM_{2.5}$ pollution in China, prohibition on open biomass burning activities has been implemented since the year 2013, causing limited activities in recent years (Huang et al., 2021, 2023). However, the open biomass burning still exist in some specific areas and time periods. During the Campaign period, we noticed more fire points during the BB period than the clean period. As shown by the satellite observations, there are obviously more fire points in the northwest and southwest of the sampling site, and the contribution of BB to $PM_{2.5}$ is also higher, with 23.2 % and 17.2 %, respectively (Fig. 7a). During the clean period, the backward trajectories were mainly marine air masses from the northeast (40.9 % from Cluster 2) (Fig. 7b), where there were fewer fire points (Fig. S16). The ocean air masses are cleaner, which facilitates the removal of pollutants. The contribution of BB to $PM_{2.5}$ in Cluster 1–4 during clean period is ranked as Cluster3 (16.6 %) > Cluster1(9.3 %) > Cluster4 (6.6 %) > Cluster2 (2.5 %) (Fig. 7b). Such results indicated that most air masses came from inside the Northeast China (NEC) plain, the Plains of the Middle and lower reaches of the Yangtze River. Therefore, regional joint prevention of BB events and controlling the pollutant emission could be an effective way to decrease the air pollution. Without considering the degradation of levoglucosan, the contribution of BB to $PM_{2.5}$ under each clustered trajectory is also underestimated based on A3 results, ranging from 2.7 % to 7.4 % in BB period and ranging from 0.8 to 5.3 % in clean period (Fig. 7 and Fig. S17).

Fig. 7c shows the potential source contribution of anhydro sugars in $PM_{2.5}$ in Changzhou during BB period. The darker color of the grid area represents a stronger contribution to the target pollutant. The potential source areas influencing Changzhou during BB period can be classified as three categories: (i) Local source areas, which are mainly located in the area bordering the provinces and cities where the receptor cities are located, i.e., cities within the YRD region. These areas distributed in the south and southeast direction of the sampling site, with their PSCF value above 0.8. (ii) Regional potential source areas, which are located in the southwestern of Changzhou, mainly including the northern cities of Jiangxi Province, such as Nanchang, with PSCF value above 0.6. (iii) Regional potential sources are located in the northern and northeastern parts of the receptor cities, with PSCF value above 0.5. During the clean period, the potential impact source areas of anhydro sugars in Changzhou mainly consisted of 2 categories: (i) Local potential source areas were located in the provinces and cities where the recipient cities were located, i.e., southern and central cities in Jiangsu Province, distributed in the north and northeast to the sampling site, with PSCF value above 0.9. (ii) regional potential sources located in the cities southwest to the recipient cities, mainly including cities in northern Jiangxi Province and southern cities in Anhui Province, with PSCF above 0.6 value above (Fig. 7d).

4. Conclusions

In this study, we observed saccharide components during 5 months in Changzhou, a typical industrialized city, which is surrounded by areas where frequent BB events occur. The average concentrations of levoglucosan, galactosan, and mannosan were 54.2 ± 80.2, 2.7 ± 3.0, and 4.3 ± 5.6 ng m^{-3}, respectively. During the observation, levoglucosan dominated the concentrations of the sugars, accounting for 80.1 %. Anhydro sugars comprised 0.88 % of organic carbon (OC). Based on

diagnostic ratio method, we found that most of BB aerosols were contributed from a mixed source of burning from wood and straw residuals. However, due to chemical degradation, approximately 87 % of levoglucosan had been degraded before sampling in Changzhou. To quantitatively analyze the influence of BB to aerosol, we conducted a multi-method comparison study, which shows that: (I) Without considering the degradation of levoglucosan would lead to an underestimation of BB to OC by 14.9 % during the whole campaign only based on the ratios of BB tracers. (II) K^+ from the ocean and dust may lead to overestimation of BB to $PM_{2.5}$, OC, and EC by 0.4 %, 1.1 %, and 0.6 %, respectively. (III) An accurate assessment of the BB contribution to aerosols could be achieved by using K^+_{BB} and considering the degradation of levoglucosan. With the addition of BB organic tracers and replaced K^+ with K^+_{BB}, the contribution of BB to $PM_{2.5}$ was enhanced by 3.2 % after considering levoglucosan degradation in PMF analysis. The underestimation of the BB contribution to $PM_{2.5}$ is quite, but under the different air mass trajectories and different periods, we noticed more fire points during the BB period than the clean period. As shown by the satellite observations, there are obviously more fire points in the northwest and southwest of the sampling site, and the contribution of BB to $PM_{2.5}$ is also higher, with 23.2 % and 17.2 %, respectively, considering the degradation of Lev.

In summary, with using K^+_{BB} and anhydro sugars, and considering the degradation of levoglucosan, an updated PMF analysis identified 6 pollution sources, including secondary aerosols (55.8 %), industrial emission (14.1 %), dust (13.6 %), biomass burning (10.7 %), coal combustion (2.4 %), and fireworks (3.4 %), with secondary aerosols have the highest contribution. Therefore, the reduction of secondary aerosol precursors is on the top priority for controlling atmospheric $PM_{2.5}$ pollution in Changzhou. During the BB period, the air mass trajectories were mainly from continental air masses of the sampling site, where there were more fire points. Given that continental air masses contribute to local pollution and oceanic air masses remove it, authorities should pay special attention to biomass burning sources and establish suitable abatement measures for the local area if it is downwind of contaminated air masses.

CRediT authorship contribution statement

Q. Li, and K. Zhang: Methodology, Investigation, Formal analysis, Writing-Original Draft.

R. Li, and LM. Yang: Methodology, Investigation, Formal analysis.

JL. Feng, W. Wang, QQ. Wang, Kasemsan Manomaiphiboon, L. Huang, YJ. Wang and M.C. Ooi: Validation.

H. Chen, SY. Wang, Andy Chan, Mohd Talib Latif: Writing-Reviewing and Editing.

JZ. Yu: Methodology, Validation, Writing-Reviewing and Editing.

L. Li: Conceptualization, Methodology, Writing-Reviewing and Editing, Funding acquisition.

Data availability

Data will be made available on request.

Declaration of competing interest

The authors declare no conflict of interest.

Acknowledgements

This study is financially supported by the National Natural Science Foundation of China (Nos. 41875161, 42075144, 42005112) and Shanghai International Science and Technology Cooperation Fund (No. 19230742500).

Appendix A. Supplementary data

Supplementary data to this article can be found online at https://doi.org/10.1016/j.scitotenv.2023.162071.

References

Altshuler, S.L., Zhang, Q., Kleinman, M.T., Garcia-Menendez, F., Moore, C.T., Hough, M.L., et al., 2020. Wildfire and prescribed burning impacts on air quality in the United States. J. Air Waste Manag. Assoc. 70, 961–970. https://doi.org/10.1080/10962247.2020.1749731.

Andreae, M.O., Merlet, P., 2001. Emission of trace gases and aerosols from biomass burning. Glob. Biogeochem. Cycles 15, 955–966. https://doi.org/10.1029/2000gb001382.

Arangio, A.M., Slade, J.H., Berkemeier, T., Poschl, U., Knopf, D.A., Shiraiwa, M., 2015. Multiphase chemical kinetics of OH radical uptake by molecular organic markers of biomass burning aerosols: humidity and temperature dependence, surface reaction, and bulk diffusion. J. Phys. Chem. A 119, 4533–4544. https://doi.org/10.1021/jp510489z.

Bai, J., Sun, X.M., Zhang, C.X., Xu, Y.S., Qi, C.S., 2013. The OH-initiated atmospheric reaction mechanism and kinetics for levoglucosan emitted in biomass burning. Chemosphere 93, 2004–2010. https://doi.org/10.1016/j.chemosphere.2013.07.021.

Bao, M.Y., Zhang, Y.L., Cao, F., Lin, Y.C., Wang, Y.H., Liu, X.Y., et al., 2021. Highly time-resolved characterization of carbonaceous aerosols using a two-wavelength Sunset thermal-optical carbon analyzer. Atmos.Meas.Tech. 14, 4053–4068. https://doi.org/10.5194/amt-14-4053-2021.

Bi, C.L., Chen, Y.T., Zhao, Z.Z., Li, Q., Zhou, Q.F., Ye, Z.L., et al., 2020. Characteristics, sources and health risks of toxic species (PCDD/Fs, PAHs and heavy metals) in $PM_{2.5}$ during fall and winter in an industrial area. Chemosphere 238. https://doi.org/10.1016/j.chemosphere.2019.124620.

Chen, H., Yin, S., Li, X., Wang, J., Zhang, R., 2018. Analyses of biomass burning contribution to aerosol in Zhengzhou during wheat harvest season in 2015. Atmos. Res. 207, 62–73. https://doi.org/10.1016/j.atmosres.2018.02.025.

Chen, J.M., Li, C.L., Ristovski, Z., Milic, A., Gu, Y.T., Islam, M.S., et al., 2017. A review of biomass burning: emissions and impacts on air quality, health and climate in China. Sci. Total Environ. 579, 1000–1034. https://doi.org/10.1016/j.scitotenv.2016.11.025.

Chen, Y.F., Xu, Y., Wang, F.Y., 2022. Air pollution effects of industrial transformation in the Yangtze River Delta from the perspective of spatial spillover. J. Geogr. Sci. 32, 156–176. https://doi.org/10.1007/s11442-021-1929-6.

Cheng, Y., Cao, X.B., Liu, J.M., Yu, Q.Q., Zhong, Y.J., Geng, G.N., et al., 2022. New open burning policy reshaped the aerosol characteristics of agricultural fire episodes in Northeast China. Sci. Total Environ. 810. https://doi.org/10.1016/j.scitotenv.2021.152272.

Cheng, Y., Engling, G., He, K.B., Duan, F.K., Ma, Y.L., Du, Z.Y., et al., 2013. Biomass burning contribution to Beijing aerosol. Atmos. Chem. Phys. 13, 7765–7781. https://doi.org/10.5194/acp- 13-7765-2013.

Deng, C.X., Tian, S., Li, Z.W., Li, K., 2022. Spatiotemporal characteristics of $PM_{2.5}$ and ozone concentrations in Chinese urban clusters. Chemosphere 295. https://doi.org/10.1016/j.chemosphere.2022.133813.

Engling, G., Carrico, C.M., Kreldenweis, S.M., Collett, J.L., Day, D.E., Malm, W.C., et al., 2006. Determination of levoglucosan in biomass combustion aerosol by high-performance anion-exchange chromatography with pulsed amperometric detection. Atmos. Environ. 40, S299–S311. https://doi.org/10.1016/j.atmosenv.2005.12.069.

Engling, G., Lee, J.J., Tsai, Y.W., Lung, S.C.C., Chou, C.C.K., Chan, C.Y., 2009. Size-resolved anhydrosugar composition in smoke aerosol from controlled field burning of rice straw. Aerosol Sci. Technol. 43, 662–672. https://doi.org/10.1080/02786820902825113.

Fabbri, D., Torri, C., Simonei, B.R.T., Marynowski, L., Rushdi, A.I., Fabianska, M.J., 2009. Levoglucosan and other cellulose and lignin markers in emissions from burning of Miocene lignites. Atmos. Environ. 43, 2286–2295. https://doi.org/10.1016/j.atmosenv.2009.01.030.

Feng, J.L., Hu, J.C., Xu, B.H., Hu, X.L., Sun, P., Han, W.L., et al., 2015. Characteristics and seasonal variation of organic matter in $PM_{2.5}$ at a regional background site of the Yangtze River Delta region,China. Atmos. Environ. 123, 288–297. https://doi.org/10.1016/j.atmosenv.2015.08.019.

Feng, X.X., Feng, Y.L., Chen, Y.J., Cai, J.J., Li, Q., Chen, J.M., 2022. Source apportionment of PM2.5 during haze episodes in Shanghai by the PMF model with PAHs. <sb:contribution><sb:title>J. Clean.</sb:title></sb:contribution><sb:host><sb:issue><sb:series><sb:title>Prod.</sb:title></sb:series></sb:issue></sb:host> 330. https://doi.org/10.1016/j.jclepro.2021.129850.

Fraser, M.P., Lakshmanan, K., 2000. Using levoglucosan as a molecular marker for the long-range transport of biomass combustion aerosols. Environ.Sci.Technol. 34, 4560–4564. https://doi.org/10.1021/es991229l.

Fu, P.Q., Kawamura, K., Chen, J., Li, J., Sun, Y.L., Liu, Y., et al., 2012. Diurnal variations of organic molecular tracers and stable carbon isotopic composition in atmospheric aerosols over Mt. Tai in the North China Plain: an influence of biomass burning. Atmos. Chem. Phys. 12, 8359–8375. https://doi.org/10.5194/acp-12-8359-2012.

Fu, P.Q., Kawamura, K., Okuzawa, K., Aggarwal, S.G., Wang, G.H., Kanaya, Y., et al., 2008. Organic molecular compositions and temporal variations of summertime mountain aerosols over Mt.Tai, North China Plain. J. Geophys. Res. Atmos. 113. https://doi.org/10.1029/2008jd009900.

Fu, P.Q., Zhuang, G.S., Sun, Y.L., Wang, Q.Z., Chen, J., Ren, L.J., et al., 2016. Molecular markers of biomass burning, fungal spores and biogenic SOA in the Taklimakan desert aerosols. Atmos. Environ. 130, 64–73. https://doi.org/10.1016/j.atmosenv.2015.10.087.

Fujii, Y., Iriana, W., Oda, M., Puriwigati, A., Tohno, S., Lestari, P., et al., 2014. Characteristics of carbonaceous aerosols emitted from peatland fire in Riau, Sumatra,Indonesia. Atmos. Environ. 87, 164–169. https://doi.org/10.1016/j.atmosenv.2014.01.037.

Fushimi, A., Saitoh, K., Hayashi, K., Ono, K., Fujitani, Y., Villalobos, A.M., et al., 2017. Chemical characterization and oxidative potential of particles emitted from open burning of cereal straws and rice husk under flaming and smoldering conditions. Atmos. Environ. 163, 118–127. https://doi.org/10.1016/j.atmosenv.2017.05.037.

Huang, L., Zhu, Y.H., Wang, Q., Zhu, A.S., Liu, Z.Y., Wang, Y.J., et al., 2021. Assessment of the effects of straw burning bans in China: emissions, air quality, and health impacts. Sci. Total Environ. 2021 (789), 147935. https://doi.org/10.1016/j.scitotenv.2021.147935.

Huang, L., Zhu, Y.H., Liu, H.Q., Wang, Y.J., et al., 2023. Assessing the contribution of open crop straw burning to ground-level ozone and associated health impacts in China and the effectiveness of straw burning bans. Environ. Int. 2023 (171), 107710. https://doi.org/10.1016/j.envint.2022.107710.

He, X., Wang, Q.Q., Huang, X.H.H., Huang, D.D., Zhou, M., Qiao, L.P., et al., 2020. Hourly measurements of organic molecular markers in urban Shanghai, China: observation of enhanced formation of secondary organic aerosol during particulate matter episodic periods. Atmos. Environ. 240. https://doi.org/10.1016/j.atmosenv.2020.117807.

Hennigan, C.J., Sullivan, A.P., Collett, J.L., Robinson, A.L., 2010. Levoglucosan stability in biomass burning particles exposed to hydroxyl radicals. Geophys. Res. Lett. 37. https://doi.org/10.1029/2010gl043088 n/a-n/a.

Hong, Y.H., Cao, F., Fan, M.Y., Lin, Y.C., Gul, C.M., Yu, M.Y., et al., 2022. Impacts of chemical degradation of levoglucosan on quantifying biomass burning contribution to carbonaceous aerosols: a case study in Northeast China. Sci. Total Environ. 819. https://doi.org/10.1016/j.scitotenv.2021.152007.

Isaacman, G., Kreisberg, N.M., Yee, L.D., Worton, D.R., Chan, A.W.H., Moss, J.A., et al., 2014. Online derivatization for hourly measurements of gas- and particle-phase semi-volatile oxygenated organic compounds by thermal desorption aerosol gas chromatography (SV-TAG). Atmos.Meas.Tech. 7, 4417–4429. https://doi.org/10.5194/amt-7-4417-2014.

Jensen, A., Liu, Z.Q., Tan, W., Dix, B., Chen, T.S., Koss, A., et al., 2021. Measurements of volatile organic compounds during the COVID-19 lockdown in Changzhou,China. Geophys. Res. Lett. 48. https://doi.org/10.1029/2021GL095560.

Jiang, P.H., Li, M.C., Sheng, Y., 2020. Spatial regulation design of farmland landscape around cities in China: a case study of Changzhou City. Cities 97. https://doi.org/10.1016/J.Cities.2019.102504.

Jung, J., Lee, S., Kim, H., Kim, D., Lee, H., Oh, S., 2014. Quantitative determination of the biomass-burning contribution to atmospheric carbonaceous aerosols in Daejeon, Korea, during the rice-harvest period. Atmos. Environ. 89, 642–650. https://doi.org/10.1016/j.atmosenv.2014.03.010.

Karar, K., Gupta, A.K., Kumar, A., Biswas, A.K., 2006. Characterization and identification of the sources of chromium, zinc, lead, cadmium, nickel, manganese and iron in PM_{10} particulates at the two sites of Kolkata, India. Environ. Monit. Assess. 120, 347–360. https://doi.org/10.1007/s10661-005-9067-7.

Karavoltsos, S., Sakellari, A., Bakeas, E., Bekiaris, G., Plavsic, M., Proestos, C., et al., 2020. Trace elements, polycyclic aromatic hydrocarbons, mineral composition, and FT-IR characterization of unrefined sea and rock salts: environmental interactions. Environ. Sci. Pollut. Res. 27, 10857–10868. https://doi.org/10.1007/s11356-020-07670-2.

Krumal, K., Mikuska, P., Vojtesek, M., Vecera, Z., 2010. Seasonal variations of monosaccharide anhydrides in PM_1 and $PM_{2.5}$ aerosol in urban areas. Atmos. Environ. 44, 5148–5155. https://doi.org/10.1016/j.atmosenv.2010.08.057.

Kumar, V., Rajput, P., Goel, A., 2018. Atmospheric abundance of HULIS during wintertime in Indo-Gangetic Plain: impact of biomass burning emissions. J. Atmos. Chem. 75, 385–398. https://doi.org/10.1007/s10874-018-9381-4.

Li, R., Wang, Q.Q., He, X., Zhu, S.H., Zhang, K., Duan, Y.S., et al., 2020. Source apportionment of $PM_{2.5}$ in Shanghai based on hourly organic molecular markers and other source tracers. Atmos. Chem. Phys. 20, 12047–12061. https://doi.org/10.5194/acp-20-12047-2020.

Li, Y.M., Fu, T.M., Yu, J.Z., Feng, X., Zhang, L.J., Chen, J., et al., 2021. Impacts of chemical degradation on the global budget of atmospheric levoglucosan and its use as a biomass burning tracer. Environ.Sci.Technol. 55, 5525–5536. https://doi.org/10.1021/acs.est.0c07313.

Liu, X.H., Zhu, B., Zhu, T., Liao, H., 2022. The seesaw pattern of $PM_{2.5}$ interannual anomalies between Beijing-Tianjin-Hebei and Yangtze River Delta across Eastern China in winter. Geophys. Res. Lett. 49. https://doi.org/10.1029/2021GL095878.

Liu, X.Y., Zhang, Y.L., Peng, Y.R., Xu, L.L., Zhu, C.M., Cao, F., et al., 2019. Chemical and optical properties of carbonaceous aerosols in Nanjing, eastern China: regionally transported biomass burning contribution. Atmos. Chem. Phys. 19, 11213–11233. https://doi.org/10.5194/acp-19-11213-2019.

Lv, M., Li, Z.Q., Jiang, Q.F., Chen, T.M., Wang, Y.Y., Hu, A.Y., et al., 2021. Contrasting trends of surface PM2.5, O3, and NO2 and their relationships with meteorological parameters in typical coastal and inland cities in the Yangtze River Delta. Int. J. Environ. Res. Public Health 18. https://doi.org/10.3390/Ijerph182312471.

Mochida, M., Kawamura, K., Fu, P.Q., Takemura, T., 2010. Seasonal variation of levoglucosan in aerosols over the western North Pacific and its assessment as a biomass-burning tracer. Atmos. Environ. 44, 3511–3518. https://doi.org/10.1016/j.atmosenv.2010.06.017.

Norris, G., Duvall, R., Brown, S., Bai, S., 2014. EPA Positive Matrix Factorization (PMF) 5.0 Fundamentals And User Guide. U.S. Environmental Protection Agency, Washington, DC EPA/600/R- 14/108 (NTIS PB2015-105147).

Ou, J.P., Hu, Q.H., Liu, H.R., Xu, S.Q., Wang, Z., Ji, X.G., et al., 2022. Exploring the impact of new particle formation events on $PM_{2.5}$ pollution during winter in the Yangtze River Delta,China. J. Environ. Sci. 111, 75–83. https://doi.org/10.1016/j.jes.2021.01.005.

Pio, C.A., Legrand, M., Alves, C.A., Oliveira, T., Afonso, J., Caseiro, A., et al., 2008. Chemical composition of atmospheric aerosols during the 2003 summer intense forest fire period. Atmos. Environ. 42, 7530–7543. https://doi.org/10.1016/j.atmosenv.2008.05.032.

Pio, C.A., Legrand, M., Oliveira, T., Afonso, J., Santos, C., Caseiro, A., et al., 2007. Climatology of aerosol composition (organic versus inorganic) at nonurban sites on a west-east transect across Europe. J. Geophys. Res.-Atmos. 112. https://doi.org/10.1029/2006JD008038.

Rajput, P., Sarin, M.M., Sharma, D., Singh, D., 2014. Organic aerosols and inorganic species from post-harvest agricultural-waste burning emissions over northern India: impact on mass absorption efficiency of elemental carbon. Environ.Sci.Process.Impacts 16, 2371–2379. https://doi.org/10.1039/C4EM00307A.

Sang, X.F., Chan, C.Y., Engling, G., Chan, L.Y., Wang, X.M., Zhang, Y.N., et al., 2011. Levoglucosan enhancement in ambient aerosol during springtime transport events of biomass burning smoke to Southeast China. Tellus B Chem. Phys. Meteorol. 63, 129–139. https://doi.org/10.1111/j.1600-0889.2010.00515.x.

Sang, X.F., Gensch, I., Laumer, W., Kammer, B., Chan, C.Y., Engling, G., et al., 2012. Stable carbon isotope ratio analysis of anhydrosugars in biomass burning aerosol particles from source samples. Environ.Sci.Technol. 46, 3312–3318. https://doi.org/10.1021/es204094v.

Sang, X.F., Zhang, Z.S., Chan, C.Y., Engling, G., 2013. Source categories and contribution of biomass smoke to organic aerosol over the southeastern Tibetan Plateau. Atmos. Environ. 78, 113–123. https://doi.org/10.1016/j.atmosenv.2012.12.012.

Shen, Z., Zhang, Q., Cao, J., Zhang, L., Lei, Y., Huang, Y., et al., 2017. Optical properties and possible sources of brown carbon in $PM_{2.5}$ over Xi'an, China. Atmos.Environ. 150, 322–330. https://doi.org/10.1016/j.atmosenv.2016.11.024.

Simoneit, B.R.T., 1999. A review of biomarker compounds as source indicators and tracers for air pollution. Environ. Sci. Pollut. Res. 6, 159–169. https://doi.org/10.1007/Bf02987621.

Suciu, L.G., Masiello, C.A., Griffin, R.J., 2019. Anhydrosugars as tracers in the earth system. Biogeochemistry 146, 209–256. https://doi.org/10.1007/s10533-019-00622-0.

Sun, H., Yang, X.H., Leng, Z.H., 2022. Research on the spatial effects of haze pollution on public health: spatial-temporal evidence from the Yangtze River Delta urban agglomerations, China. Environ. Sci. Pollut. Res. https://doi.org/10.1007/s11356-022-19017-0.

Tang, H.Q., Jiang, P.H., Du, H.Y., Cheng, Q.W., Li, M.C., 2022. Evaluation of municipal territorial utilisation quality in new-type urbanisation: a case study of Changzhou, China. Appl.Spat.Anal.Policy https://doi.org/10.1007/s12061-022-09474-y.

van Drooge, B.L., Fontal, M., Bravo, N., Fernandez, P., Fernandez, M.A., Munoz-Arnanz, J., et al., 2014. Seasonal and spatial variation of organic tracers for biomass burning in PM_1 aerosols from highly insolated urban areas. Environ. Sci. Pollut. Res. 21, 11661–11670. https://doi.org/10.1007/s11356-014-2545-0.

Vicente, E.D., Vicente, A., Evtyugina, M., Carvalho, R., Tarelho, L.A.C., Oduber, F.I., et al., 2018. Particulate and gaseous emissions from charcoal combustion in barbecue grills. Fuel Process. Technol. 176, 296–306. https://doi.org/10.1016/j.fuproc.2018.03.004.

Wang, Q.Q., He, X., Zhou, M., Huang, D.D., Qiao, L.P., Zhu, S.H., et al., 2020. Hourly measurements of organic molecular markers in urban Shanghai, China: primary organic aerosol source identification and observation of cooking aerosol aging. ACS EarthSpace Chem. 4, 1670–1685. https://doi.org/10.1021/acsearthspacechem.0c00205.

Wang, Y.Q., Zhang, X.Y., Draxler, R.R., 2009. TrajStat: GIS-based software that uses various trajectory statistical analysis methods to identify potential sources from long-term air pollution measurement data. Environ. Model Softw. 24, 938–939. https://doi.org/10.1016/j.envsoft.2009.01.004.

White, W.H., 2008. Chemical markers for sea salt in IMPROVE aerosol data. Atmos. Environ. 42, 261–274. https://doi.org/10.1016/j.atmosenv.2007.09.040.

Williams, B.J., Goldstein, A.H., Kreisberg, N.M., Hering, S.V., 2006. An in-situ instrument for speciated organic composition of atmospheric aerosols: Thermal Desorption Aerosol GC/MS-FID (TAG). Aerosol Sci. Technol. 40, 627–638. https://doi.org/10.1080/02786820600754631.

Williams, B.J., Goldstein, A.H., Millet, D.B., Holzinger, R., Kreisberg, N.M., Hering, S.V., et al., 2007. Chemical speciation of organic aerosol during the International Consortium for Atmospheric Research on Transport and Transformation 2004: results from in situ measurements. J. Geophys. Res.-Atmos. 112. https://doi.org/10.1029/2006JD007601.

Xiao, M.X., Wang, Q.Z., Qin, X.F., Yu, G.Y., Deng, C.R., 2018. Composition, sources, and distribution of $PM_{2.5}$ saccharides in a coastal urban site of China. Atmosphere 9. https://doi.org/10.3390/Atmos9070274.

Xu, S.F., Ren, L.J., Lang, Y.C., Hou, S.J., Ren, H., Wei, L.F., et al., 2020. Molecular markers of biomass burning and primary biological aerosols in urban Beijing: size distribution and seasonal variation. Atmos. Chem. Phys. 20, 3623–3644. https://doi.org/10.5194/acp-20-3623-2020.

Yan, C.Q., Sullivan, A.P., Cheng, Y., Zheng, M., Zhang, Y.H., Zhu, T., et al., 2019. Characterization of saccharides and associated usage in determining biogenic and biomass burning aerosols in atmospheric fine particulate matter in the North China Plain. Sci. Total Environ. 650, 2939–2950. https://doi.org/10.1016/j.scitotenv.2018.09.325.

Yan, C.Q., Zheng, M., Sullivan, A.P., Shen, G.F., Chen, Y.J., Wang, S.X., et al., 2018. Residential coal combustion as a source of levoglucosan in China. Environ.Sci.Technol. 52, 1665–1674. https://doi.org/10.1021/acs.est.7b05858.

Yang, C., Hong, Z.Y., Chen, J.S., Xu, L.L., Zhuang, M.Z., Huang, Z., 2022. Characteristics of secondary organic aerosols tracers in $PM_{2.5}$ in three central cities of the Yangtze river delta, China. Chemosphere 293. https://doi.org/10.1016/j.chemosphere.2022.133637.

Ye, Z.L., Liu, J.S., Gu, A.J., Feng, F.F., Liu, Y.H., Bi, C.L., et al., 2017. Chemical characterization of fine particulate matter in Changzhou, China, and source apportionment with offline aerosol mass spectrometry. Atmos. Chem. Phys. 17, 2573–2592. https://doi.org/10.5194/acp-17-2573-2017.

Zhang, K., Yang, L.M., Li, Q., Li, R., Zhang, D.P., Xu, W., et al., 2021. Hourly measurement of PM2.5-bound nonpolar organic compounds in Shanghai: characteristics, sources and health risk assessment. Sci. Total Environ. 789. https://doi.org/10.1016/j.scitotenv.2021.148070.

Zhang, T., Cao, J.J., Chow, J.C., Shen, Z.X., Ho, K.F., Ho, S.S., et al., 2014. Characterization and seasonal variations of levoglucosan in fine particulate matter in Xi'an, China. J. Air Waste Manag. Assoc. 64, 1317–1327. https://doi.org/10.1080/10962247.2014.944959.

Zhang, Y.X., Shao, M., Zhang, Y.H., Zeng, L.M., He, L.Y., Zhu, B., et al., 2007. Source profiles of particulate organic matters emitted from cereal straw burnings. J. Environ. Sci. 19, 167–175. https://doi.org/10.1016/S1001-0742(07)60027-8.

Zhu, C., Kawamura, K., Kunwar, B., 2015. Effect of biomass burning over the western North Pacific Rim: wintertime maxima of anhydrosugars in ambient aerosols from Okinawa. Atmos. Chem. Phys. 15, 1959–1973. https://doi.org/10.5194/acp-15-1959-2015.

Zhu, S.H., Wang, Q.Q., Qiao, L.P., Zhou, M., Wang, S., Lou, S.R., et al., 2021. Tracer-based characterization of source variations of $PM_{2.5}$ and organic carbon in Shanghai influenced by the COVID-19 lockdown. Faraday Discuss. 226, 112–137. https://doi.org/10.1039/d0fd00091d.